Journal of Photochemistry and Photobiology A: Chemistry 199 (2008) 250–254

Contents lists available at ScienceDirect

Journal of Photochemistry and Photobiology A: Chemistry

journal homepage: www.elsevier.com/locate/jphotochem

Photo-catalysis using titanium dioxide nanotube layers

K.O. Awitor[a,*], S. Rafqah[a], G. Géranton[a], Y. Sibaud[a], P.R. Larson[b], R.S.P. Bokalawela[b], J.D. Jernigen[b], M.B. Johnson[b]

[a] Institut Universitaire de Technologie, Département Mesures Physiques, Université d'Auvergne, 63172 Aubière Cedex, France
[b] Homer L. Dodge Department of Physics and Astronomy, University of Oklahoma, Norman, OK 73019, USA

ARTICLE INFO

Article history:
Received 22 February 2008
Received in revised form 27 May 2008
Accepted 30 May 2008
Available online 11 June 2008

Keywords:
Titanium dioxide nanotubes
Anatase
Rutile
Photo-degradation
Acid orange 7 (AO7)
Mineralization

ABSTRACT

Photo-degradation of acid orange 7 in aqueous solution was used as a probe to assess the photo-catalytic activity of titanium dioxide nanotube layers under UV irradiation. The nanotube layers were prepared by anodization of Ti foil in 0.4 wt% hydrofluoric acid solution and then annealed at different temperatures between 300 °C and 600 °C for 1 h. The nanotube layers were characterized using X-ray diffraction and scanning electron microscopy. After the 500 °C anneal, the anatase and rutile mass fractions were measured to be about 55% and 45%, respectively. After annealing at 500 °C, the anatase crystallite size was maximum while the size and shape of the nanotubes remain unaffected. Such TiO_2 nanotube layers showed strong photo-catalytic activity. During UV irradiation, we measured the total disappearance of the organic carbon and the formation of anion species to confirm the total mineralization of the acid orange 7.

1. Introduction

Titanium dioxide (TiO_2) is a photo-catalytic material with applications in fields such as environmental purification, decomposition of carbonic acid gases, and solar cells [1–7]. Several techniques can be used to prepare TiO_2 thin films, including thermal oxidation of titanium and sputtering [8–13]. TiO_2 nanotube layers grown by anodic oxidation of Ti foils in an appropriate electrolyte provide ordered nanotube arrays with high surface area to volume ratios [14–17]. Such layers have attracted much attention, including recent work on wetting behaviour [18], oxygen adsorption [19], and heterogeneous photo-catalysis [14]. One of the most active research areas has been focused on environmental remediation, including self-cleaning materials. For example, TiO_2-based photo-catalysts have been used to break down organic compounds in wastewater [1,3,5]. Indeed, many organic pollutants can be degraded and ultimately mineralized using TiO_2 photo-catalysts in the presence of UV radiation [14,20–25]. Recently, there have been studies investigating the degradation of organic solutions using TiO_2 nanotube layers [4,14]. The nanotube layers give rise to a large specific surface area and this should produce a greater photo-catalytic activity for a given sample size. In this work, we assess the photo-catalytic activity of TiO_2 nanotube layers by monitoring the degradation of an acid orange 7 (AO7) dye solution. The TiO_2 nanotube layers were annealed in an oxygen atmosphere at different temperatures. The study of structural evolution versus annealing temperature performed by X-ray diffraction shows that at 500 °C the anatase and the rutile mass fractions are around 55% and 45%, respectively. At this temperature, the size of the anatase crystallites was maximum and the TiO_2 nanotubes demonstrated strong photo-catalytic activity under UV irradiation. Scanning electron microscopy (SEM) was used to study the nanotube morphology. Finally, we show that the photo-catalytic activity of TiO_2 nanotube layers leads to the total mineralization of AO7.

2. Experimental details

To fabricate anodic TiO_2 nanotube layers, we used Ti foil (Goodfellow, 99.6% purity) with a thickness of 0.025 mm. The Ti foils were degreased by successive sonication in trichloroethylene, acetone, and methanol, followed by rinsing with deionized water and blown dry with nitrogen. Anodization was carried out at room temperature (20 °C) in 0.4 wt% HF aqueous solution with the anodizing voltage maintained at 20 V.

The crystalline structure and phase of the TiO_2 nanotube layers were determined using a Scintag XRD X'TRA diffractometer with Cu Kα radiation. A JEOL JSM-880 SEM was used for morphological characterization.

* Corresponding author. Tel.: +33 4 73 17 71 66; fax: +33 4 73 17 71 71.
E-mail address: awitor@iut.u-clermont1.fr (K.O. Awitor).

1010-6030/$ – see front matter © 2008 Elsevier B.V. All rights reserved.
doi:10.1016/j.jphotochem.2008.05.023

Photo-degradation of AO7 in aqueous solution was used as a probe to assess the photo-catalytic activity of TiO_2 nanotube layers. Photo-catalytic experiments were conducted in 15 mL of AO7 solution (from Acros Organics, also called Orange II, CAS# 633-96-5) with a concentration of 5.0×10^{-5} mol/L, placed in a cylindrical Pyrex glass reactor (1.1 cm diameter by 18 cm tall). The surface area of the anodized samples was approximately 6.5 cm^2. The glass reactor was irradiated with polychromatic fluorescent UV lamps (Philips TDL 8 W (total optical power, 1.3 W), 300 mm long, wavelength range 350–400 nm) in a configuration providing about 2 mW/cm^2 at the sample surface.

The photo-catalytic decomposition of AO7 solution was monitored by the decrease of the solution's absorbance at 254 nm (centered in an absorption band of the AO7 solution), using a Merck high-performance liquid chromatography (HPLC) system. This HPLC system was equipped with a mono-channel (L-7400) UV–vis detector, an automatic injector (L7200) and pump (L7100). Experiments to investigate the decomposition of AO7 under UV irradiation into smaller organic molecules were performed using a reverse phase Interchrom column (Hypersil H_5C_{18}, 150 mm long × 4.6 mm diameter) to analyze the solution. The flow rate of AO7 solution was 1.0 mL/min and the injected volume was 10 μL. The elution was accomplished by water with ammonium acetate (25×10^{-3} mol/L) and acetonitrile (75/25, v/v) with a flow rate of 1.0 mL/min. We followed the evolution of the 485 nm band of the irradiated solution using a UV–vis and IR spectrometer (Shimadzu UV-2101). The progress of the mineralization of AO7 solution was monitored by measuring the total organic carbon (TOC) using a Shimadzu Model TOC-5050A system, equipped with an automatic sample injector. The calibration curve within the range 1–15 mg/L was obtained by using potassium hydrogen phthalate, $KC_8H_5O_4$, and sodium hydrogen carbonate, $NaHCO_3$, for organic and inorganic carbon, respectively. The evolution of nitrate, nitrite and sulphate ion concentrations was obtained as a function of irradiation time using a Dionex, DX-100, ionic chromatography system. The elution was accomplished using Na_2CO_3 (1.8×10^{-3} mol/L)/$NaHCO_3$ (1.7×10^{-3} mol/L) with a flow rate of 2.0 mL/min.

3. Results and discussion

3.1. TiO_2 nanotube layer characteristics

Fig. 1 shows SEM images of the TiO_2 nanotubes obtained by anodizing a Ti foil. We observe ordered nanotube arrays grown on top of the Ti foil with an oxide barrier layer separating the nanotubes from the titanium foil. Fig. 1(a) shows the top down image of the ordered array of TiO_2 nanotubes in the unannealed state approximately 100 nm in diameter. Fig. 1(b) shows an oblique view of the unannealed TiO_2 nanotubes (55° from normal). The tube length determined by accounting for foreshortening from this image was found to be approximately 430 nm. Fig. 1(c and d) shows top and oblique views after annealing at 500 °C. Comparing before and after views, we see no difference in the micrographs. Thus the size and shape of the nanotubes are not affected by the 500 °C anneal.

Fig. 2 summarizes the X-ray characterization of Ti foil and TiO_2 nanotube layers before and after annealing at different temperatures in oxygen for 1 h. The unannealed TiO_2 nanotube layer exhibits only the peaks from titanium metal foil under the nanotube layer. In order to convert the nanotube layer to a crystalline phase, the samples were annealed at 300–600 °C in increments of 50 °C. The characteristic line of anatase (1 0 1) appears at 300 °C, while the rutile line (1 1 0) appears at 500 °C. These lines are shown in more detail in Fig. 2(b). Crystallite size was calculated using the Scherrer formula, $D = 0.94\lambda/\beta \cos\theta$, where λ is the wavelength of the Cu $K\alpha_1$ line, θ is the Bragg diffraction angle, and β is the full-width at half max (FWHM) of a peak. We calculated the crystallite size

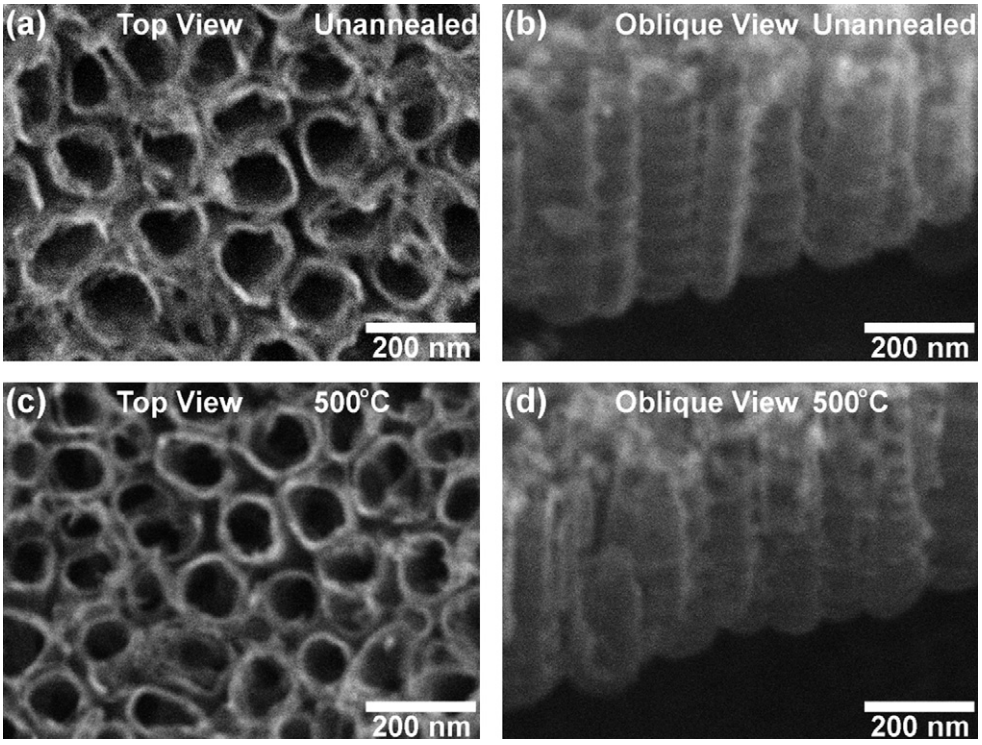

Fig. 1. SEM images of TiO_2 nanotubes obtained by anodizing Ti foil. (a) Top view image of the ordered array of unannealed TiO_2 nanotubes showing typical diameter to be about 100 nm. (b) Oblique view (55° from normal) of the unannealed TiO_2 nanotubes showing tube length of about 430 nm. (c) Top view of TiO_2 nanotube array annealed at 500 °C. (d) Oblique view (55° from normal) of TiO_2 nanotube array at 500 °C.

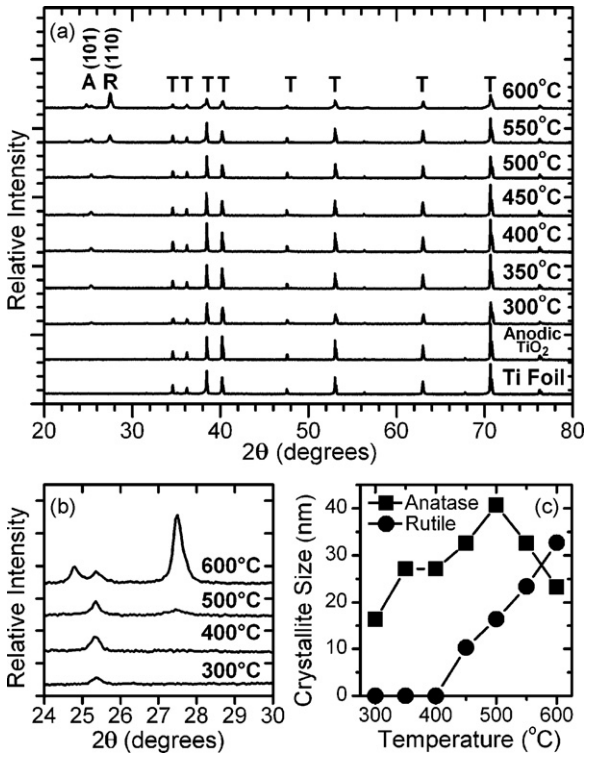

Fig. 2. (a) X-ray diffraction patterns of Ti foil, as grown and annealed TiO_2 nanotube layers. Annealing temperatures are marked. Lattice planes indicate anatase (A), rutile (R), and titanium (Ti). (b) Evolution of the (1 0 1) anatase, and (1 1 0) rutile lines at 300–600 °C. (c) Peak heights of (1 0 1) anatase and (1 1 0) rutile lines, and crystallite size for anatase and rutile phases (calculated using Sherrer's formula) versus temperature.

evolution by using the FWHM of the anatase (1 0 1) and the rutile (1 1 0) peaks. Fig. 2(c) is a plot of crystallite size versus temperature. We found that the size of anatase grows from 17 nm to 40 nm as the annealing temperature is increased from 300 °C to 500 °C. The rutile crystallite size was 17 nm at 500 °C. After 500 °C, the anatase peak decreases significantly while the rutile peak increases. At 500 °C the anatase-to-rutile mass ratio was around 55:45. The anatase-to-rutile mass ratio decreased to 30:70 and further to 20:80 after one-hour annealing at 550 °C and 600 °C, respectively. It is interesting to note, that even after annealing at 500 °C the size and shape of the nanotubes are not observed to change, while the crystalline structure clearly does change. This is in agreement with the results described by Varghese et al. [15] and Macak et al. [14].

3.2. Photo-catalytic activity study

The photo-degradation of AO7 in the presence of TiO_2 nanotubes under different conditions is summarized in Fig. 3. This shows the AO7 concentration versus time as determined by the solution's absorbance at 254 nm. As shown in Fig. 4, a plot of absorption versus wavelength, 254 nm is at the center of an AO7 absorption band. For Fig. 3, the initial concentration of the AO7 was 5.0×10^{-5} mol/L. Fig. 3, curve (a) shows the photo-degradation of AO7 under UV light without TiO_2 present. This result indicates that AO7 is not substantially degraded by UV radiation alone. Curve (b) shows that the reduction in the concentration of AO7 in the presence of TiO_2 nanotubes for 40 h without UV irradiation was about 20%. Thus, the effect of adsorption of the dye on the TiO_2 surface is small but not negligible. Curve (c) shows the variation in the concentration of AO7 in the presence of unannealed TiO_2 nanotubes under UV irradiation. Here we only observe the adsorption effect. Curves (d), (e) and

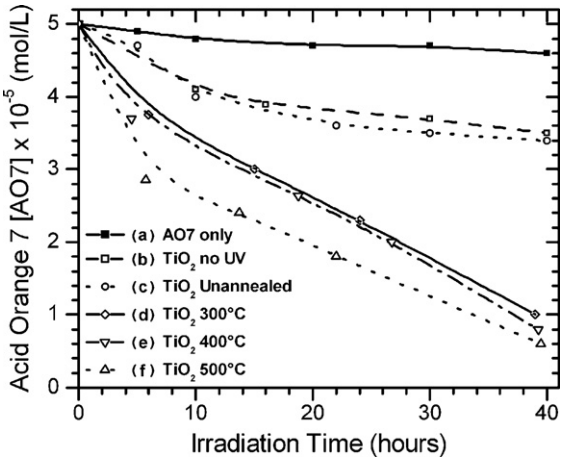

Fig. 3. Photo-degradation of acid orange 7 (AO7) dye under UV-lamp irradiation at wavelengths of 350–400 nm in the presence of TiO_2 nanotube layer, as measured by the absorbance of the irradiated dye at 254 nm. (a) AO7 only with UV; (b) AO7 with TiO_2 nanotube layer without UV; (c) unannealed TiO_2 nanotube layer; (d) TiO_2 nanotube layer annealed at 300 °C; (e) TiO_2 nanotube layer annealed at 400 °C; (f) TiO_2 nanotube layer annealed at 500 °C.

(f) illustrate photo-degradation of AO7 after the samples had been annealed at 300 °C, 400 °C and 500 °C, respectively. We observed a complete de-colorization of the AO7 dye after 40 h. These results show the decay of organic molecules with UV irradiation in the presence of the annealed nanotubes.

We observed the strongest photo-catalytic activity for the sample annealed at 500 °C. In this case, the kinetics are first order with a rate constant of about 0.05 h^{-1}. At this temperature the anatase-to-rutile mass fraction is about 55:45 and the anatase crystallite size of 40 nm was maximum. It seems that the TiO_2 nanotube layers show strong photo-catalytic activity when composed of mixed crystalline phases (anatase and rutile) with excess anatase. This behaviour is similar to that for the crystalline powder Degussa P25, which exhibits a strong photo-catalytic activity and has an anatase-to-rutile mass fraction of 80:20. Our results are in agreement with those observed by Macak et al. [14] for the de-colorization of AO7 dye. The difference in the rate constant of Macak et al. compared to our rate constant (0.63 h^{-1} vs. 0.05 h^{-1}) is due to differences in their experiment to our experiment: nanotube length (0.5 μm vs.

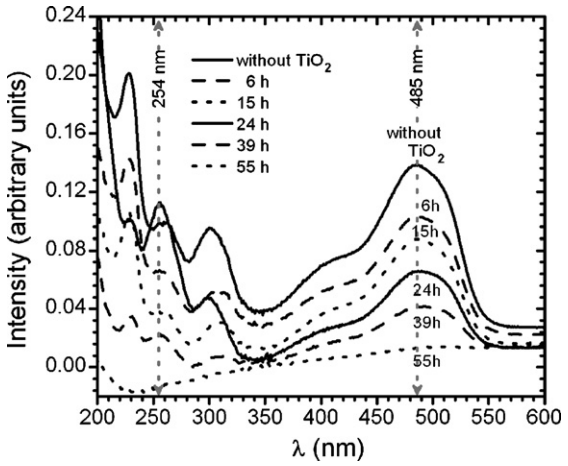

Fig. 4. Absorption versus irradiation time for the acid orange 7 (AO7) for polychromatic light (350–400 nm) without TiO_2 nanotube layers, and in the presence of TiO_2 nanotube layers annealed at 300 °C with exposure times of 6 h, 15 h, 24 h, 39 h, and 55 h, as labelled.

0.43 μm), illuminated sample area (1 cm^2 vs. 6.5 cm^2), intensity at the sample (60 mW/cm^2 vs. 2 mW/cm^2), and AO7 volume (3 mL vs. 15 mL). In detail, taking our rate constant of 0.05 h^{-1} and converting it to the experimental situation of Macak et al., we expect a rate constant of 0.05 $h^{-1} \times (0.5/0.43) \times (1/6.5) \times (60/2)/(3/15)$, or 1 h^{-1}, which is in reasonable agreement with Macak's rate constant of 0.63 h^{-1} (see [26]).

It is useful to compare the photo-catalytic activity of this TiO_2 nanotube surface with other TiO_2 surfaces. Macak et al. compares the activity of a similar nanotube surface to a standard preparation of Degussa P25 powder and finds comparable activity for equal illuminated sample areas (0.63 h^{-1} vs. 0.50 h^{-1}). This indicates that the TiO_2 nanotube surface is promising. Comparing our TiO_2 nanotube surface to an optimized sputter-deposited TiO_2 surface [27] (sputtered from a Ti target in a reactive Ar–O_2 gas mixture) we find similar rate constants, even though the sputtered TiO_2 surface has a lower specific area in comparison. This implies the photocatalytic activity of the surface of the TiO_2 nanotubes is lower than that of an optimized sputtered surface, indicating there is room for improvement in the activity of the surface of the TiO_2 nanotubes.

Fig. 4 shows typical UV–vis spectra obtained during UV irradiation of AO7 in the presence of the TiO_2 nanotubes annealed at 300 °C. (Results for nanotube layers annealed at the higher temperatures are similar.) These spectra clearly show that the intensity of the characteristic band of AO7 at 485 nm decreases as a function of irradiation time, so that after 50 h of irradiation the AO7 solution is colorless.

Mineralization of AO7 was studied by following the disappearance of the total organic carbon (TOC), as shown in Fig. 5. The formation of anion species (nitrites, nitrates, and sulphates) was followed by using ionic liquid chromatography during irradiation. Fig. 5 shows that the TiO_2 nanotube structure is efficient at eliminating the AO7 dye in aqueous solution. During the UV irradiation, a rapid decrease in the number of carbon atoms was observed corresponding to the scission and oxidation of AO7.

Conversely, Fig. 6 shows the increase of the concentration of anions (formed after mineralization) with irradiation time. The chemical formula for AO7 is $HOC_{10}H_6N{=}NC_6H_4SO_3Na$, so there is one sulphur atom and two nitrogen atoms for every AO7 molecule. Regarding sulphur, the concentration of sulphates reaches a plateau of about 4.7 mg/L or 4.9×10^{-5} mol/L. Given the starting concentration of AO7 is 5.0×10^{-5} mol/L, essentially all (98%) of the sulphur in the starting AO7 is converted into sulphates. Regarding nitrogen, the formation of the nitrate and nitrite ions reached a plateau in concentration of 0.6 mg/L or 1×10^{-5} mol/L, and 0.1 mg/L or 0.2×10^{-5} mol/L, respectively. Taking into account the two N atoms in AO7, 10% (2%) of the nitrogen ends up as nitrate (nitrite). This suggests the remaining 88% of the nitrogen forms N_2 [20,24] and/or ammonium ions that are not directly tracked [21,25].

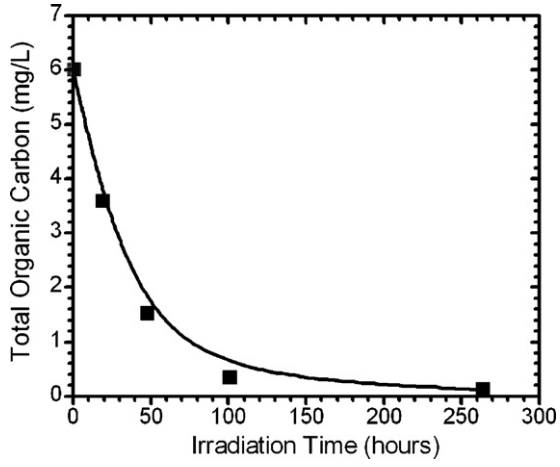

Fig. 5. The evolution of total organic carbon (TOC) of acid orange 7 (AO7) dye (starting concentration 5.0×10^{-5} mol/L) versus irradiation time in the presence of a TiO_2 nanotube layer annealed at 500 °C.

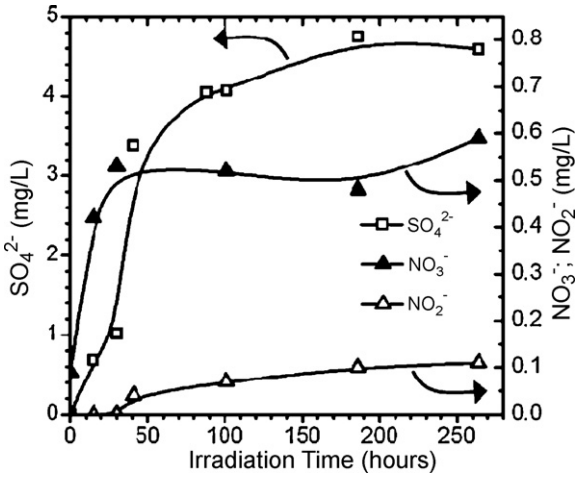

Fig. 6. Formation of inorganic anions, nitrates, nitrites, and sulphates, upon UV irradiation of AO7 dye in the presence of a TiO_2 nanotube layer annealed at 500 °C.

4. Conclusions

Photo-degradation and the mineralization capacity of TiO_2 nanotube layers were studied using AO7 in aqueous solution as a probe. Anodization of Ti foil results in ordered arrays of TiO_2 nanotubes. The TiO_2 nanotube layers annealed at 500 °C for 1 h in oxygen show strong photo-catalytic activity, in agreement with earlier studies [14]. After this anneal, X-ray diffraction indicated the nanotube layer is composed of mixed crystalline phases (anatase and rutile) with an excess of anatase in agreement with the earlier work [14–16]. For the nanotube layer annealed at 500 °C we observe the breakdown of AO7 by following the absorption of the UV-irradiated solution at 254 nm. Complete de-colorization of the AO7 dye was observed after 40 h. The mineralization of the AO7 was confirmed by direct measurement of the reduction of total organic carbon, and by the direct measurement of the increase in the concentration of sulphate, nitrate and nitrite anions in the UV-irradiated solution.

References

[1] S.-A. Lee, K.-H. Choo, C.H. Lee, H.-I. Lee, T. Hyeon, W. Choi, H.-H. Kwon, Ind. Eng. Chem. Res. 40 (2001) 1712.
[2] W. Choi, Catal. Surv. Asia 10 (2006) 16.
[3] J. Ryu, W. Choi, Environ. Sci. Technol. 42 (2008) 294.
[4] G.K. Mor, M.A. Carvalho, O.K. Varghese, M.V. Pishko, C.A. Grimes, J. Mater. Res. 19 (2004) 628.
[5] Y. Xiong, P.J. Strunk, H. Xia, X. Zhu, H.T. Karlsson, Water Res. 35 (2001) 4226.
[6] T. Kasuga, M. Hiramatsu, M. Hirano, A. Honson, K. Oyamada, J. Mater. Res. 12 (1997) 607.
[7] M.R. Hoffmann, S.T. Martin, W. Choi, D.W. Bahnemann, Chem. Rev. 95 (1995) 69.
[8] I. Saeki, N. Okushi, H. Konno, R. Furuichi, J. Electrochem. Soc. 143 (1996) 2226.
[9] B. Karunagaran, R.T.R. Kumar, D. Mangalaraj, S.K. Narayandass, G.M. Rao, Cryst. Res. Technol. 37 (2002) 1285.
[10] M.C. Barnes, S. Kumar, L. Green, N.-M. Hwang, A.R. Gerson, Surf. Coat. Technol. 190 (2005) 321.
[11] P. Hoyer, H. Masuda, J. Mater. Sci. Lett. 15 (1996) 1228.
[12] S.-Z. Chu, K. Wada, S. Inoue, S.-I. Todoroki, Chem. Mater. 14 (2002) 266.
[13] H. Imai, Y. Takei, K. Shimizu, M. Matsuda, H. Hirashima, J. Mater. Chem. 9 (1999) 2971.
[14] J.M. Macak, M. Zlamal, J. Krysa, P. Schmuki, Small 3 (2007) 300.

[15] O.K. Varghese, D. Gong, M. Paulose, C.A. Grimes, E.C. Dickey, J. Mater. Res. 18 (2003) 156.
[16] D. Gong, C.A. Grimes, O.K. Varghese, W. Hu, R.S. Singh, Z. Chen, E.C. Dickey, J. Mater. Res. 16 (2001) 3331.
[17] V. Zwilling, M. Aucouturier, E. Darque-Ceretti, Electrochim. Acta 45 (1999) 921.
[18] E. Balaur, J.M. Macak, H. Tsuchiya, P. Schmuki, J. Mater. Chem. 15 (2005) 4488.
[19] S. Funk, B. Hokkanen, U. Burghaus, A. Ghicov, P. Schmuki, Nano Lett. 7 (2007) 1091.
[20] M.A. Behnajady, N. Modirshahla, N. Daneshvar, M. Rabbani, Chem. Eng. J. 127 (2007) 167.
[21] K. Tanaka, K. Padermpole, T. Hisanaga, Water Res. 34 (2000) 327.
[22] E. Vulliet, C. Emmelin, J.-M. Chovelon, C. Guillard, J.-M. Herrmann, Environ. Chem. Lett. 1 (2003) 62.
[23] J. Fernández, J. Kiwi, J. Baeza, J. Freer, C. Lizama, H.D. Mansilla, Appl. Catal. B Environ. 48 (2004) 205.
[24] H. Lachheb, E. Puzenat, A. Houas, M. Ksibi, E. Elaloui, C. Guillard, J.-M. Herrmann, Appl. Catal. B Environ. 39 (2002) 75.
[25] H. Kyung, J. Lee, W. Choi, Environ. Sci. Technol. 39 (2005) 2376.
[26] The experimental rate constant, determined by the decrease in AO7 concentration, should be proportional to tube length, sample area, and UV intensity, while inversely proportional to the volume of the A07 solution. Actually, Macak et al. see diminishing improvement with longer tube length, but this is not important here because the difference in nanotube lengths is very small.
[27] K.O. Awitor, A. Rivaton, J.-L. Gardette, A.J. Down, M.B. Johnson, Thin Solid Films 516 (2008) 2286.